



# Influence of Multifrequency Ultrasound-Assisted Freezing on the Flavour Attributes and Myofibrillar Protein Characteristics of Cultured Large Yellow Croaker (*Larimichthys crocea*)

Xuan Ma<sup>1</sup>, Dazhang Yang<sup>1,2,3,4</sup>, Weiqiang Qiu<sup>1,2,3,4</sup>, Jun Mei<sup>1,2,3,4\*</sup> and Jing Xie<sup>1,2,3,4\*</sup>

<sup>1</sup> College of Food Science and Technology, Shanghai Ocean University, Shanghai, China, <sup>2</sup> National Experimental Teaching Demonstration Center for Food Science and Engineering Shanghai Ocean University, Shanghai, China, <sup>3</sup> Shanghai Engineering Research Center of Aquatic Product Processing and Preservation, Shanghai, China, <sup>4</sup> Shanghai Professional Technology Service Platform on Cold Chain Equipment Performance and Energy Saving Evaluation, Shanghai, China

## OPEN ACCESS

### Edited by:

Emmanuel Purlis,  
Consejo Nacional de Investigaciones  
Científicas y Técnicas  
(CONICET), Argentina

### Reviewed by:

Md. Nahidul Islam,  
Bangabandhu Sheikh Mujibur Rahman  
Agricultural University, Bangladesh  
Baoguo Xu,  
Jiangsu University, China

### \*Correspondence:

Jun Mei  
jmei@shou.edu.cn  
Jing Xie  
jxie@shou.edu.cn

### Specialty section:

This article was submitted to  
Nutrition and Food Science  
Technology,  
a section of the journal  
Frontiers in Nutrition

**Received:** 19 September 2021

**Accepted:** 15 November 2021

**Published:** 15 December 2021

### Citation:

Ma X, Yang D, Qiu W, Mei J and Xie J  
(2021) Influence of Multifrequency  
Ultrasound-Assisted Freezing on the  
Flavour Attributes and Myofibrillar  
Protein Characteristics of Cultured  
Large Yellow Croaker (*Larimichthys*  
*crocea*). *Front. Nutr.* 8:779546.  
doi: 10.3389/fnut.2021.779546

The influence of multifrequency ultrasound-assisted freezing (UAF) as compared with single- and dual-UAF on the flavour, microstructure, and myofibrillar proteins (MPs) of cultured large yellow croaker was investigated to improve food quality in a sustainable way and address the major global challenges concerning food and nutrition security in the (near) future. Multifrequency UAF-treated samples had lower total volatile basic nitrogen values during freezing than single- and dual-UAF-treated samples. Thirty-six volatile compounds were identified by solid-phase microextraction (SPME) coupled to gas chromatography–mass spectrometry (GC-MS) during freezing, and the multifrequency UAF-treated samples showed significant decreases in the relative contents of fishy flavoured compounds, including 1-penten-3-ol and 1-octen-3-ol. In addition, multifrequency UAF treatment better maintained a well-organised protein secondary structure by maintaining higher  $\alpha$ -helical and  $\beta$ -sheet contents and stabilising the tertiary structure. Scanning electron microscopy images indicated that the ice crystals developed by the multifrequency UAF were fine and uniformly distributed, resulting in less damage to the frozen large yellow croaker samples. Therefore, multifrequency UAF improved the flavour attributes and MP characteristics of the large yellow croaker samples. Overall, multifrequency UAF can serve as an efficient way for improving food quality and nutritional profile in a sustainable way.

**Keywords:** large yellow croaker, multi-frequency ultrasound assisted freezing, microstructure, flavour attributes, myofibrillar protein characteristics

## INTRODUCTION

Large yellow croaker (*Larimichthys crocea*) is an important marine cultured fish that is widely distributed in China. Freezing is an efficient method to extend the shelf life of large yellow croaker by controlling microbial growth and decreasing biochemical reactions (1). The quality of frozen fish is affected by the size of the ice crystals and their location within the fish (2). The size and

homogeneity of ice crystals are largely affected by the freezing rate. Generally, rapid freezing can produce fine and uniform extra- and intracellular ice crystals that cause less damage to food structures. In contrast, slow freezing generates large and uneven extracellular ice crystals, which can damage the muscle structure and decrease the quality of the food (3). Several innovative and emerging freezing techniques have been used to provide a promising means to optimise the crystallisation of frozen fish. These techniques, including radio frequency-assisted freezing (4), high-pressure freezing (5), and ultrasound-assisted freezing (UAF) (6–11) can change the nucleation, nucleation rate, and crystal growth of food substrates during freezing.

Ultrasound-assisted freezing has a favourable effect on the process of food freezing due to its cavitation effects (12, 13). The movement of cavitation bubbles can lead to a microstreaming effect, thus improving the efficiency of heat and mass transfer (14). Furthermore, cavitation bubbles can serve as crystal nuclei and increase the number of nucleation sites. Large ice crystals can be fragmented by microstreaming, resulting in a further decrease in the size of ice crystals (15). Some studies have indicated that ultrasound facilitates the freezing processes of different food materials. Sun et al. (16) evaluated the effects of UAF with different ultrasound powers on myofibrillar protein (MP) structures and the thermal stability of common carp and found that ultrasound treatment at 175 W significantly reduced the changes in protein structure and preserved the thermal stability of the protein during freezing. Single-frequency ultrasounds have been frequently used in the freezing investigations mentioned above. The frequency is closely associated with the intensity of ultrasonic cavitation and is an important indicator of the acoustic-chemical reaction (17). It also has an impact on the bubble activity induced by the bubble rupture, which has an impact on the product quality. The coupling of ultrasonic energy peaks when the natural resonant frequency of the bubble is commensurate with the ultrasonic frequency (18). Compared to single-frequency ultrasound, multifrequency ultrasound has been indicated to greatly improve cavitation effects (19). Ma et al. (20) proposed that the effect of dual-frequency flat ultrasound is more significant than that of single-frequency flat ultrasound because of its homogeneous energy dissipation over a broader region. The efficiency of various acoustic and cavitation devices, such as dual frequency and single frequency devices, was investigated by Jawale et al. (21). They pointed out that dual-frequency acoustic-chemical reactors show more effective performance during use than single-frequency acoustic-chemical reactors. Wang et al. (22) investigated the influence of multifrequency ultrasound-assisted thawing on the structure and rheological characteristics of MPs in small yellow croaker and found that dual-frequency ultrasonic thawing could effectively minimise the changes in structure and preserve the rheological characteristics of MPs compared with single-frequency ultrasonic thawing.

We are currently and will continue to face major global challenges concerning food and nutrition security. It is expected that stresses to food systems continue to appear in the (near) future, for example, pandemics, economic shocks, and climate change effects at local and global scales. As previously stated,

much progress has been made regarding the ultrasound-assisted immersion freezing of food materials, since it was first reported ~20 years ago (23). However, many studies on freezing fish products by ultrasound remain in their infancy, and the majority still adopt single-frequency ultrasound for freezing. To the best of our knowledge, there are few studies on the application of multifrequency UAF in food materials. Considering these backgrounds, this study was designed to disseminate solutions based on multifrequency UAF, an innovative and emerging non-thermal food engineering technology, to build sustainable and resilient food systems, improve nutritional profile of foods, and increase food and nutrition security. This study evaluated the changes in total volatile basic nitrogen (TVB-N), scanning electron microscopy (SEM) observations, flavour attributes, free amino acids (FAAs), and MP characteristics of large yellow croaker samples frozen by multifrequency ultrasound (consisting of single-, dual-, and triple-frequency ultrasound).

## MATERIALS AND METHODS

### Sample Preparation

Fresh large yellow croakers (weighing  $550 \pm 25$  g) were purchased from a local market in Luchao Port town (Shanghai, China). The fresh fish were prepared by a local processor, and the viscera and gills were removed. Then, the treated fish were transported to our laboratory on ice within 30 min and washed with saline solution containing 0.9% sodium chloride.

### Freezing Process

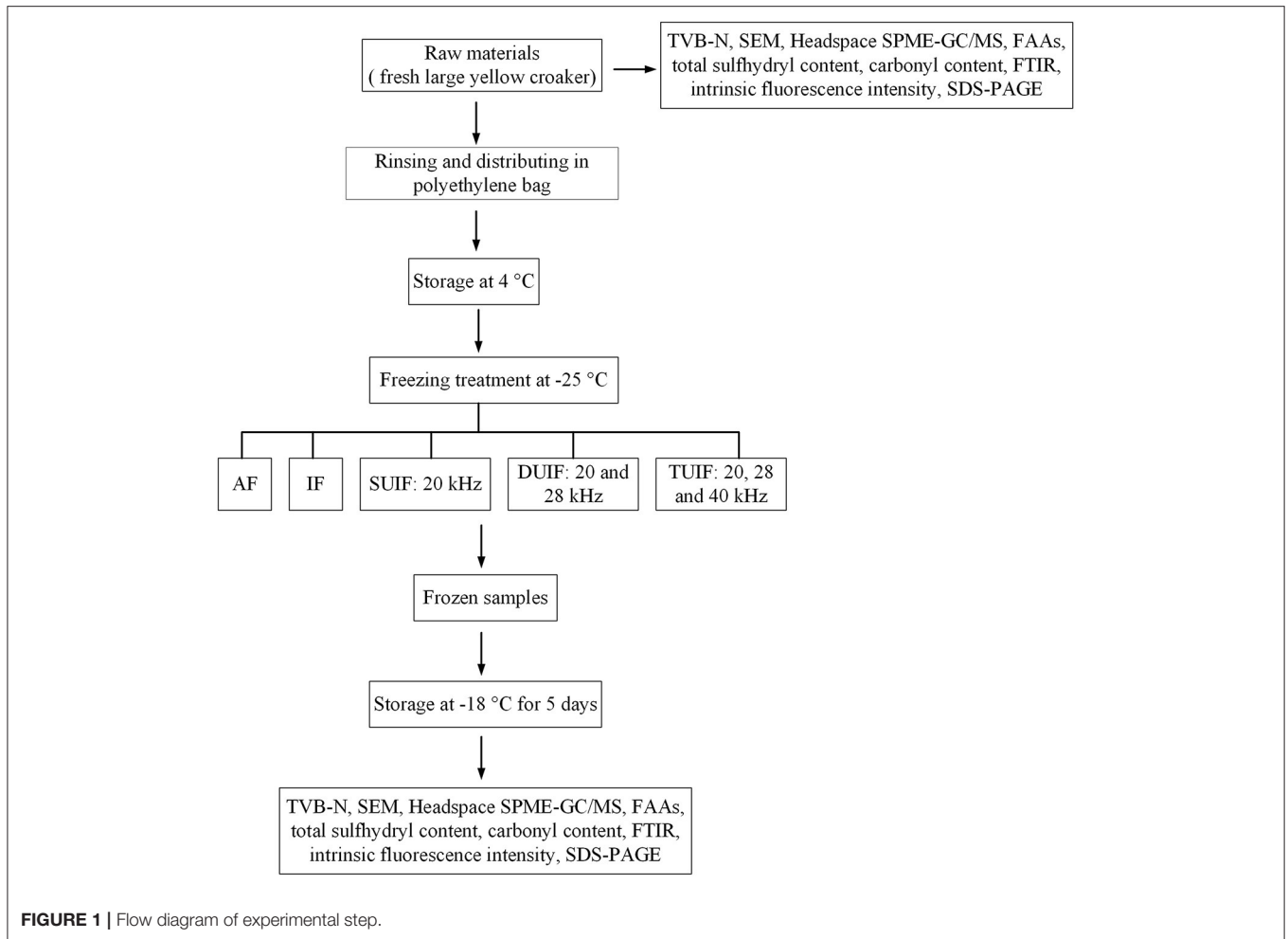
According to the experimental procedure of Ma et al. (24), the fish samples were subjected to the following five different freezing treatments: air freezing (AF), immersed freezing (IF), and ultrasound-assisted immersed freezing (UIF) linked with single frequency at 20 kHz (SUIF), UIF linked with dual frequency at 20/28 kHz (DUIF), and ultrasound-assisted immersed freezing linked with triple frequency at 20/28/40 kHz (TUIF). The multifrequency ultrasound-assisted freezer was customised by Xiecheng Ultrasonic Equipment Co., Ltd. (Jining, Shandong, China). This system used 29.3% calcium chloride brine solution (w/v) as the coolant. The temperature of coolant was set to  $(-25.0 \pm 0.5)^\circ\text{C}$  with a cryogenic circulation pump. A detailed flow diagram of the experimental procedure is presented in **Figure 1**. A diagram of the multifrequency ultrasound-assisted immersion freezing unit is presented in **Figure 2**.

### Evaluation of TVB-N

Total volatile basic nitrogen values were examined with a Kjeldahl apparatus (Kjeltec8400, Foss, Hilleroed, Denmark). The results of TVB-N are shown as mg N/100 g of large yellow croaker samples (25).

### SEM Observation

The morphology of frozen dorsal muscle samples was observed by SEM according to the procedure proposed by Xu et al. (17) with minor modifications. The freeze-dried large yellow croaker samples were placed on one surface of a two-sided adhesive tape and coated with a thin gold layer; then the morphology of the



fish samples was observed by extreme-resolution analytical field emission SEM (Mira 3 XH, Tescan, Brno, Czech Republic). For the SEM observation, the acceleration voltage was 5 kV.

### Analysis of Headspace by Solid Phase Microextraction and Gas Chromatography–Mass Spectrometry

Volatile organic compounds (VOCs) of samples under different freezing conditions were separated and detected using the procedure proposed by Li et al. (26). A 2-g mashed large yellow croaker sample and 5 ml of 25%  $\text{NaH}_2\text{PO}_4$  solution were mixed and placed in a 20 ml headspace vial. The VOCs were characterized *via* comparison with commercial reference compounds obtained from Sigma–Aldrich (St. Louis, MO, USA), and their mass spectra were compared with those included in the NIST 2011.

### Analysis of FAAs

Free amino acids were determined using the method proposed by Yu et al. (27). A 2-g chopped large yellow croaker sample and 10 ml of 5% cold trichloroacetic acid were mixed and homogenised at  $10,000 \times g$  for 10 min. The extraction and centrifugation were repeated and the combined supernatants

were diluted to 25 ml. The supernatant was filtered through a  $0.22 \mu\text{m}$  filter. An automatic amino acid analyser (Hitachi L-8800, Tokyo, Japan) was used for evaluation.

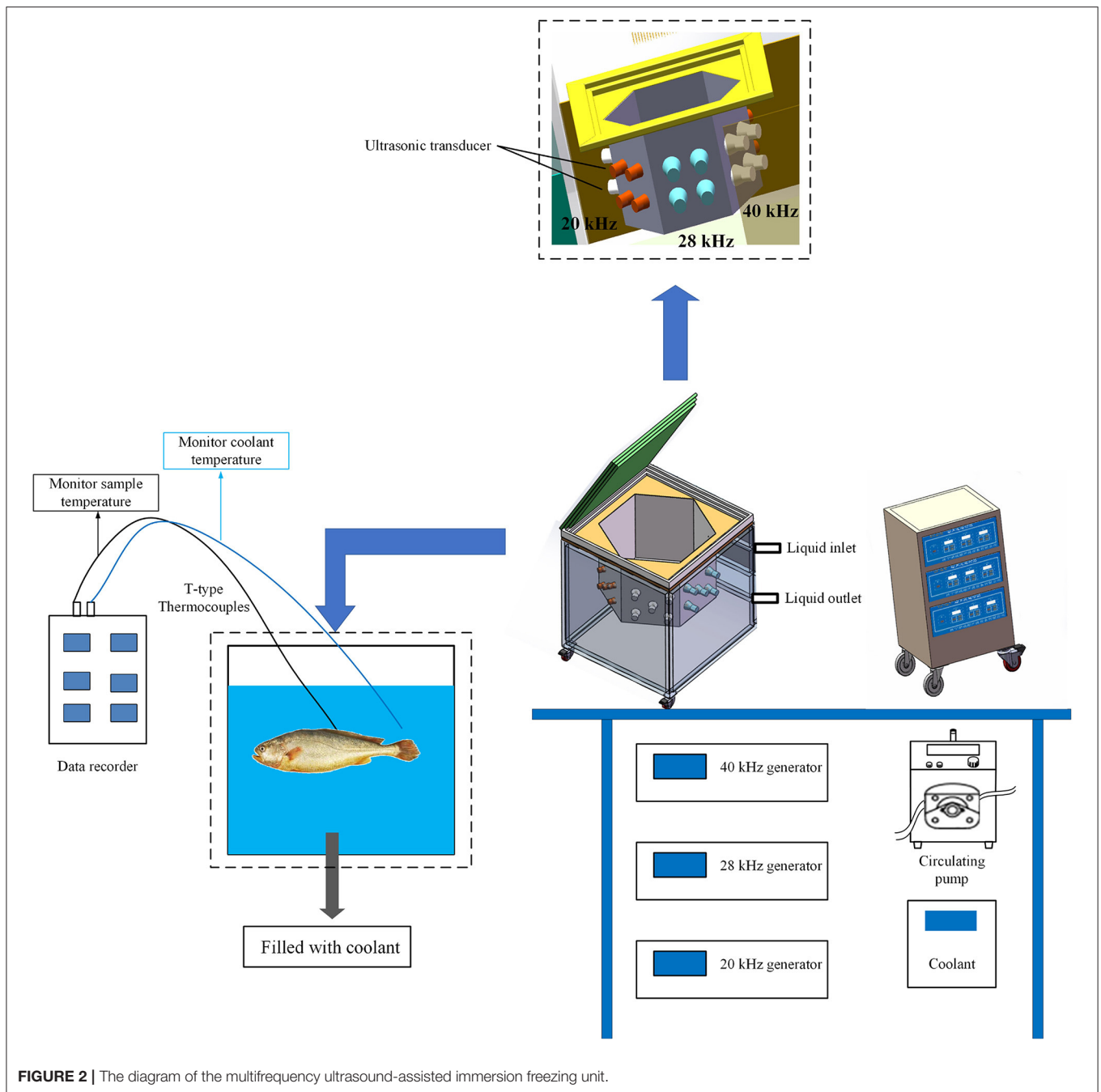
### Extraction of MP

Myofibrillar protein was obtained as proposed by Guo et al. (28) with minor modifications. In short, 2 g of minced large yellow croaker flesh was mixed with 20 ml of prechilled Tris-buffer A (0.05 M KCl, 20 mM Tris-maleate, pH 7.0) and homogenised in an ice bath for 30 s. The mixture was then centrifuged at 10,000 r/min and  $4^\circ\text{C}$  for 15 min and the precipitate was retained. The above homogenisation and centrifugation steps were repeated twice, and the precipitate was mixed with 20 ml of prechilled Tris-buffer B (0.6 M NaCl, 20 mM Tris-maleate, pH 7.0). After that, the mixture was homogenised in an ice bath for 30 s and left for 3 h. The supernatant was obtained as a myofibrillar protein solution by centrifugation at 10,000 r/min and  $4^\circ\text{C}$  for 15 min. The solutions were kept frozen at  $-40^\circ\text{C}$  until further analysis.

### MP Primary Structure

#### Determination of Total Sulfhydryl Content

The total sulfhydryl content was measured by the procedure proposed by Li et al. (29) with slight modifications. A 1 g dorsal



muscle large yellow croaker flesh sample was homogenised in 10 ml of an 8 M urea solution mixed with 0.6 M NaCl. Afterwards, the mixture was centrifuged at 2,500 g/min at 4°C for 10 min. Then, 0.5 mL of the supernatant was combined with 4.5 ml of buffer A (8 M urea, 3 mM EDTA, 1% SDS, 0.2 M Tris-HCl, pH 8.0) and mixed homogeneously. Subsequently, 0.625 mL of buffer B (10 mM DTNB, 10 mM Tris-HCl, pH 8.0) was supplemented, and the mixture was maintained at 40°C for 20 min. The absorbance was measured at a wavelength of 405 nm at room temperature,

and colorimetry was completed within 30 min. The final calculated value of total sulfhydryl content is given as  $\mu\text{mol/g}$  protein.

#### Determination of Carbonyl Content

The carbonyl group content was evaluated using derivatisation with 2,4-dinitrophenyl hydrazine according to the method described by Zhang et al. (30). The carbonyl groups reacted with 2,4-dinitrophenylhydrazine to produce protein hydrazone. The results are given as nmol/mg protein.

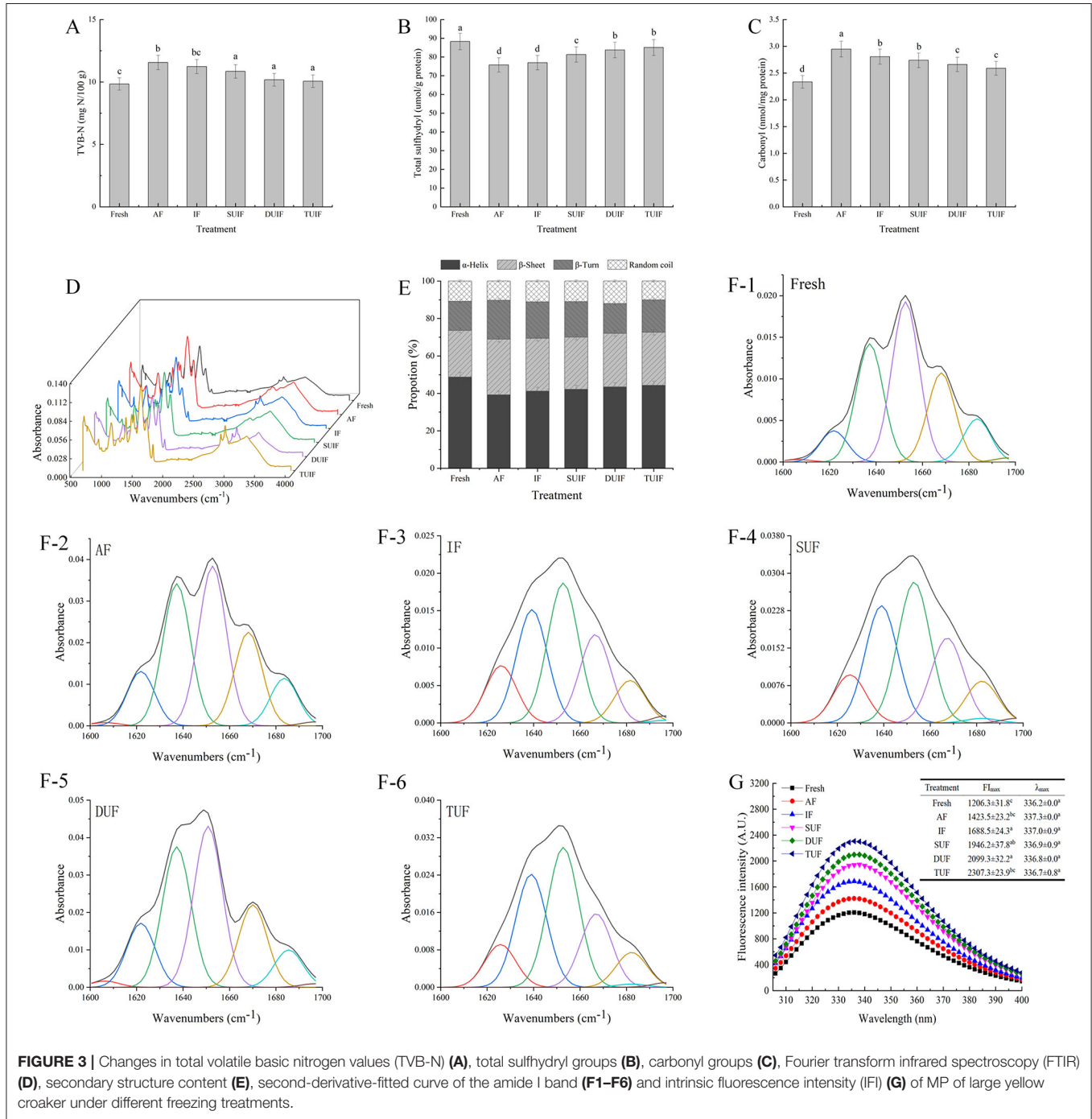
### MP Secondary Structure

The secondary structure of the MP solution was determined by Fourier transform infrared (FTIR) spectroscopy. The dried myofibril sample was ground with potassium bromide powder to form a uniform powder. Then, it was pressed into a sheet, and the secondary structure was measured using a Fourier infrared spectrometer (Nicolet IS50; Thermo Scientific Inc., Waltham, MA, USA). The test parameters were as follows: the scanning

wavelength range was 4,500–500  $\text{cm}^{-1}$ , the resolution was 4  $\text{cm}^{-1}$ , and the number of scans was 32 (31).

### MP Tertiary Structure

The intrinsic fluorescence intensity (IFI) of extracted myofibril samples was measured using an AFS-9230 fluorescence spectrophotometer (Beijing Titan Instruments Co., Ltd., China). The acquisition parameters are shown below. The emission



spectra range was 300–400 nm and the scanning speed was 1,200 nm/min. The maximum fluorescence wavelength ( $\lambda_{max}$ ) of the fluorescence emission spectrum was documented (29).

## Statistical Analysis

SPSS 22.0 software was used to statistically evaluate the experimental results which are reported as the means  $\pm$  standard deviation. Significant differences ( $p < 0.05$ ) in the mean values of treatments were determined using the one-way ANOVA and Duncan's multiple range tests.

## RESULTS AND DISCUSSION

### Total Volatile Basic Nitrogen

Total volatile basic nitrogen quantifies alkaline volatile compounds, including ammonia, trimethylamine, methylamine, dimethylamine, and so on, which is the primary parameter for evaluating the variation in freshness of aquatic products (32). The TVB-N content of the fresh large yellow croaker samples was 9.84 mg N/100 g (Figure 3A). The TVB-N values in the AF- and IF-treated samples were higher than those in the UAF sample. AF and IF treatment can form large ice crystals through slow freezing to puncture the cells, increase the amount of water in the extracellular space, and cause nutrient leakage, which provides a suitable culture environment for microorganisms and results in an increase in TVB-N in fish (33, 34). A significant difference among the samples with UIF treatments was not observed ( $p > 0.05$ ), and the lowest TVB-N values were found in the TUIF-treated samples (10.85, 10.18, and 10.06 mg N/100 g for the SUIF, DUIF, and TUIF samples, respectively). The possible reason behind this is that the higher operating frequency of triple-frequency ultrasound overcomes the disadvantages of single-frequency and dual-frequency ultrasound, such as non-uniform energy consumption per unit volume and directional sensitivity. In addition, triple-frequency ultrasound can produce more cavitation bubbles and resonances named “combination resonances,” as well as greater sonochemical energy (35). The TVB-N values of the TUIF samples were reduced by 12.98 and 10.50% compared with that of the IF and AF samples, respectively, suggesting that rapid freezing can diminish the generation of TVB-N in fish samples. Sun et al. (36) also stated that the TVB-N of common carp samples after UAF treatments was less than that of samples after AF and IF treatment.

### Scanning Electron Microscopy

The SEM images of large yellow croaker muscle (cross-section and longitudinal section) under different freezing treatments are shown in Figures 4A,B. The pores in the SEM images are connected with the location and size of ice crystals. The largest pore size was observed for the AF-treated samples compared with the other samples. The microstructure of large yellow croaker frozen by UIF was better than that of the samples frozen under AF and IF. The microstructure of TUIF samples was found to be the most compact and had the smallest holes, indicating that TUIF treatment resulted in the smallest and most uniformly distributed ice crystals among the fish samples. The multifrequency ultrasonic treatments resulted in a reduction

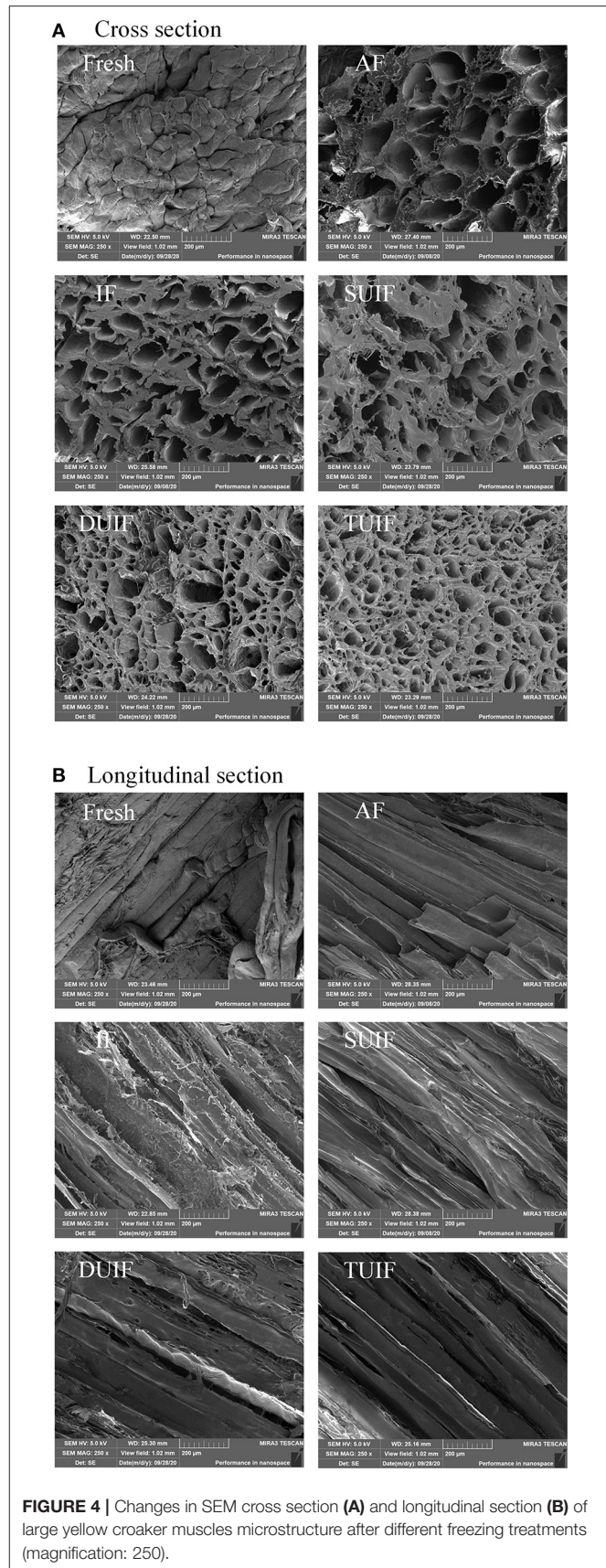


**FIGURE 4** | Changes in SEM cross section (A) and longitudinal section (B) of large yellow croaker muscles microstructure after different freezing treatments (magnification: 250).

in the size of ice crystals developed during the freezing of samples. The mechanism for small ice crystal formation can be roughly divided into three points. (i) A higher freezing rate and shorter phase transition time can contribute to the rapid conversion of freezable moisture into ice crystals (11, 37); (ii) large dendritic ice crystals can be broken into small fragments,

consequently enhancing secondary nucleation (38, 39); and (iii) cavitation bubbles can be applied as crystal nuclei once they attain the critical size of ice nucleation, leading to an increase in nucleation sites (10, 15). Zhu et al. (40) also observed that the ice crystals generated by the TUIF and DUIF treatments were finer and more homogeneously distributed on potato samples. It has

**TABLE 1** | Retention index and area of main volatile compounds identified in large yellow croaker under different freezing treatment.

Name	Treatments						
	RI	Fresh	AF	IF	SUIF	DUIF	TUIF
<b>Alcohols</b>							
1-Octanol	1,560.6	ND	$1.83 \times 10^5$	ND	ND	$1.24 \times 10^5$	ND
1,4-Butanediol	1,926.2	$1.03 \times 10^6$	$4.08 \times 10^5$	$1.30 \times 10^5$	$6.69 \times 10^4$	$3.55 \times 10^5$	ND
Ethanol	930.16	$7.91 \times 10^5$	$1.20 \times 10^6$	$8.38 \times 10^6$	$8.37 \times 10^6$	$7.53 \times 10^6$	$9.96 \times 10^6$
3-Methyl-2-butanol	1,123.7	$9.57 \times 10^5$	$3.13 \times 10^5$	$5.57 \times 10^4$	$4.01 \times 10^5$	ND	ND
2-Decanol	1,143.1	$4.82 \times 10^5$	$2.65 \times 10^4$	$2.98 \times 10^5$	$3.51 \times 10^5$	ND	$4.34 \times 10^5$
1-Butanol	1,164.7	$2.14 \times 10^6$	$6.20 \times 10^6$	ND	ND	$2.52 \times 10^6$	$1.22 \times 10^5$
1-Penten-3-ol	1,173.5	$2.39 \times 10^6$	$3.65 \times 10^6$	$3.37 \times 10^6$	$3.16 \times 10^6$	$3.05 \times 10^6$	$2.70 \times 10^6$
3-Methyl-1-butanol	1,218.5	$1.87 \times 10^6$	$5.96 \times 10^6$	ND	ND	ND	ND
2-Methyl-1-butanol	1,216.6	$1.07 \times 10^5$	ND	ND	ND	ND	ND
1-Pentanol	1,258.2	$5.58 \times 10^5$	$1.50 \times 10^6$	$4.29 \times 10^5$	$5.03 \times 10^5$	$6.17 \times 10^5$	$4.23 \times 10^5$
2-n-Propyl-1-heptanol	1,283.1	$6.34 \times 10^5$	$1.88 \times 10^6$	$3.58 \times 10^5$	$5.59 \times 10^5$	$4.53 \times 10^6$	$8.07 \times 10^5$
1-Hexanol	1,356.5	$4.60 \times 10^5$	$1.40 \times 10^7$	$5.65 \times 10^5$	$3.23 \times 10^6$	ND	$5.16 \times 10^5$
1-Octen-3-ol	1,450	$1.27 \times 10^6$	$8.60 \times 10^6$	$1.68 \times 10^6$	$1.45 \times 10^6$	$1.45 \times 10^6$	$1.37 \times 10^6$
2-Ethyl-1-hexanol	1,490.2	$3.96 \times 10^5$	$5.22 \times 10^6$	$2.18 \times 10^6$	$7.10 \times 10^5$	$8.79 \times 10^5$	$8.06 \times 10^5$
<b>Aldehydes</b>							
Propanal	852.24	$5.37 \times 10^6$	$1.25 \times 10^5$	$1.04 \times 10^7$	$6.65 \times 10^7$	$1.16 \times 10^7$	$6.85 \times 10^5$
Butanal	885.36	$4.65 \times 10^4$	$1.22 \times 10^5$	$1.51 \times 10^5$	$9.14 \times 10^4$	$7.86 \times 10^4$	$6.28 \times 10^4$
2-Methyl-butanal	908.29	$7.57 \times 10^5$	$1.60 \times 10^5$	ND	$1.86 \times 10^5$	ND	$1.55 \times 10^5$
3-Methyl-butanal	911.27	$1.81 \times 10^6$	$1.42 \times 10^6$	ND	$1.69 \times 10^5$	$4.37 \times 10^4$	$1.77 \times 10^5$
Pentanal	969.23	$1.25 \times 10^6$	$1.40 \times 10^7$	$1.17 \times 10^6$	$1.34 \times 10^6$	$1.16 \times 10^6$	$9.71 \times 10^5$
Hexanal	1,076	$1.16 \times 10^7$	$8.67 \times 10^5$	$9.19 \times 10^6$	$1.06 \times 10^7$	$9.35 \times 10^6$	$7.65 \times 10^6$
Heptanal	1,172	$5.65 \times 10^5$	ND	ND	$3.16 \times 10^6$	$4.55 \times 10^6$	$2.70 \times 10^6$
Octanal	1,277.6	$5.48 \times 10^5$	$1.84 \times 10^6$	ND	$5.08 \times 10^5$	$5.34 \times 10^5$	$6.26 \times 10^5$
Nonanal	1,384.6	$9.64 \times 10^5$	ND	$9.73 \times 10^5$	$1.40 \times 10^6$	$1.17 \times 10^6$	$1.13 \times 10^6$
(E, E)-2,4-Heptadienal	1,485.9	$3.96 \times 10^5$	$2.37 \times 10^6$	ND	ND	ND	ND
Benzaldehyde	1,511.4	$3.31 \times 10^7$	ND	ND	$1.10 \times 10^6$	$1.87 \times 10^6$	$2.49 \times 10^6$
<b>Ketones</b>							
Acetone	859.89	$2.68 \times 10^4$	ND	$3.81 \times 10^4$	$3.46 \times 10^4$	$3.82 \times 10^4$	$3.39 \times 10^4$
Methyl Isobutyl Ketone	1,003.7	$1.96 \times 10^5$	$7.71 \times 10^6$	ND	ND	$2.09 \times 10^5$	$1.26 \times 10^5$
2,3-Pentanedione	1,055.2	$2.04 \times 10^5$	$6.99 \times 10^6$	$5.72 \times 10^6$	$4.53 \times 10^6$	$3.97 \times 10^6$	$3.18 \times 10^6$
1-(p-Tolyl) butan-1-one	1,933.1	$1.27 \times 10^6$	ND	$8.11 \times 10^4$	$8.25 \times 10^5$	$4.73 \times 10^7$	$4.48 \times 10^5$
2-Butanone	899.58	ND	ND	ND	$2.89 \times 10^5$	$6.07 \times 10^5$	$7.22 \times 10^5$
3-hydroxy-2-butanone	1,283.4	ND	$6.80 \times 10^5$	$1.45 \times 10^6$	$1.06 \times 10^6$	$1.31 \times 10^6$	$6.52 \times 10^5$
<b>Esters</b>							
Ethyl Acetate	891.73	$1.50 \times 10^5$	$4.89 \times 10^6$	ND	$5.32 \times 10^5$	$2.81 \times 10^5$	$5.64 \times 10^5$
n-Caproic acid vinyl ester	1,315.9	$2.69 \times 10^6$	ND	ND	$2.10 \times 10^6$	$2.25 \times 10^6$	ND
Monolaurin	1,835.7	ND	$1.78 \times 10^5$	ND	ND	$1.79 \times 10^5$	ND
Methyl acetoacetate	1,123.7	ND	ND	$1.87 \times 10^6$	$3.63 \times 10^4$	$6.89 \times 10^5$	ND
<b>Others</b>							
2-Ethylfuran	941.63	$3.52 \times 10^6$	$2.77 \times 10^6$	$3.31 \times 10^6$	$4.20 \times 10^6$	$3.64 \times 10^6$	$3.22 \times 10^6$

ND, not detected.

been reported that multifrequency ultrasound can significantly enhance the cavitation effect in contrast to single-frequency ultrasound (41). Jin et al. (42) stated that multifrequency ultrasound pretreatment can enhance the enzymolysis of corn gluten meal under various enzymolysis conditions. Nevertheless, the mechanism of action of multifrequency ultrasound has not been intensively investigated. The potential mechanisms are primarily the reinforcement of mechanical perturbations and the augmentation of cavitation nuclei associated with multifrequency ultrasound (41).

## Volatile Compounds

In total, thirty-six major VOCs were characterised from the large yellow croaker samples throughout for the whole freezing process, without considering aromatic compounds, hydrocarbons, and amine components. As presented in **Table 1**, these VOCs included alcohols, aldehydes, ketones, esters, and other compounds.

Fourteen alcohol compounds were characterised, and the levels of 1-octen-3-ol and 2-ethyl-1-hexanol showed a certain increase during the freezing process. 1-penten-3-ol, ethanol, 1-pentanol, 2-*n*-propyl-1-heptanol, 1-octen-3-ol, and 2-ethyl-1-hexanol exhibited relatively high abundance during the whole freezing process of the large yellow croaker samples. Among them, 1-penten-3-ol is regarded as a highly essential volatile substance possessing green, vegetal, and burnt flavour descriptors, which has been suggested to be an indicator of lipid oxidation in chilled Atlantic horse mackerel meat (43). Furthermore, 1-octen-3-ol is a significant provider of off-flavours because of its low odour threshold. 1-Penten-3-ol and 1-octen-3-ol in the samples with UIF treatment exhibited lower abundances than those in the samples with AF and IF treatment. The levels of 1-penten-3-ol in SUIF-, DUIF-, and TUIF-treated samples were reduced by 13.42, 16.44, and 26.03% compared with AF-treated samples, respectively, and by 6.23, 9.50, and 19.88% compared with IF-treated samples, respectively. The levels of 1-octen-3-ol in the SUIF-, DUIF-, and TUIF-treated samples decreased by 83.14, 83.14, and 84.07% compared with AF-treated samples, respectively, and by 13.69, 13.69, and 18.45% compared with IF-treated samples, respectively. In particular, the levels of 1-penten-3-ol and 1-octen-3-ol in the TUIF-treated sample were similar to those in the fresh samples. The triple-frequency ultrasound can produce obviously higher improvement in cavitation yield in comparison with the single-frequency and dual-frequency ultrasound. In addition, the triple-frequency ultrasound showed more combination resonances, which can generate a much broader range of bubble sizes compared with the single-frequency and dual-frequency ultrasound (44). TUIF treatment generated small and homogeneously distributed ice crystals in the muscle tissue *via* a comparatively quick-freezing rate, which better protected the cell properties and caused the muscles to be of great quality. In addition, UIF efficiently inhibited both the action of 15-lipoxygenase on EPA (20:5n-3) and of 12-lipoxygenase on arachidonic acid (45).

Aldehyde compounds are principally derived from the oxidation of polyunsaturated fatty acids. Generally, aldehydes containing three to four carbon atoms generate strongly irritating

odours, while those containing five to nine carbon atoms generate a lipidic aroma. In some cases, the Strecker degradation of amino acids can produce aldehydes. For instance, benzaldehyde is obtained through the degradation of phenylglycine, as a pleasant fruity almond-like aroma in large yellow croaker (46). Benzaldehyde showed higher relative concentrations in the fresh samples, which is in accordance with the study performed by Tan et al. (47). However, benzaldehyde was not observed in the AF and IF samples, which could be due to a greater degree of lipid oxidation as a result of severe damage to the muscle structure. Benzaldehyde, as well as octanal and heptanal, have been characterised as components of the aroma of fresh fish (48). The occurrence of 2,4-heptadienal may be attributed to the autoxidation of eicosapentaenoic acid (20:5 $\omega$ -3) (EPA) (49).

Ketone compounds were found at relatively low levels and exerted less of an effect on the flavour than aldehydes. Among ketones, increases in 3-hydroxy-2-butanone and 2,3-pentanedione levels occurred, the latter serving as an index of lipid oxidation in the muscles of frozen fish. 2,3-Pentanedione exhibited a lower abundance in the UIF-treated samples than in the AF- and IF-treated samples. The levels of 2,3-pentanedione in the SUIF-, DUIF-, and TUIF-treated samples were reduced by 35.19, 43.20, and 54.51% compared with the AF-treated samples, respectively, and by 20.80, 30.59, and 44.41% compared with the IF-treated samples, respectively. Specially, the levels of 2,3-pentanedione in the TUIF-treated sample ( $3.18 \times 10^6$ ) were nearly the same as those in the fresh samples. TUIF treatment better protected the cell structure, thereby improving muscle quality. In addition, UIF efficiently inhibited lipid oxidation by decreasing the activities of lipase, phospholipase, and lipoxygenase (50). 3-Hydroxy-2-butanone was detected only after freezing treatment and is regarded as a potential indicator of marine fish. The formation of 3-hydroxy-2-butanone is mainly associated with lactic acid bacteria (51). VOCs derived from lipid autoxidation are recognised as the main factors for the quality deterioration of fish. In terms of the changes in VOCs, the peak areas of the off-odour compounds in samples were lower after UIF treatment, indicating that UAF inhibited lipid oxidation.

## FAAs Analysis

Free amino acids are essential factors involved in the flavour development of aquatic products. The taste properties of FAAs are dependent on the structures of the functional groups and side chain R groups. Most D-amino acids are mainly sweet; Met, Gly, Thr, Ala, and Ser with short side chains are mainly sweet and umami; and Tyr, Phe, Ile, Val, and Leu with large and long side chains are mainly bitter (52). Significant differences ( $p < 0.05$ ) were observed in the total FAA contents among all samples during the freezing process. The total FAA levels in the UAF and IF samples were notably higher than those in the AF samples. The increase in FAA content is a consequence of the decomposition of proteins and peptides caused by proteolytic enzymes, while its reduction is a consequence of the interaction of those amino acids with other compounds and the loss of water-soluble FAAs during thawing. Fast freezing can effectively decrease the thawing loss of large yellow croaker, resulting in the highest value of total FAAs (112.00 mg/100 g) in TUIF



**TABLE 2** | Changes in free amino acids (FAAs) content (mg/100 g) of large yellow croaker muscles after different freezing treatments.

Samples	FAAs								
	Asp	Thr	Ser	Glu	Gly	Ala	Val	Met	
Fresh	0.83 ± 0.01 <sup>e</sup>	2.63 ± 0.04 <sup>f</sup>	3.65 ± 0.05 <sup>f</sup>	6.67 ± 0.11 <sup>d</sup>	7.69 ± 0.11 <sup>f</sup>	20.74 ± 0.22 <sup>b</sup>	6.58 ± 0.07 <sup>a</sup>	3.21 ± 0.02 <sup>a</sup>	
AF	0.99 ± 0.01 <sup>d</sup>	3.07 ± 0.04 <sup>e</sup>	4.90 ± 0.06 <sup>c</sup>	7.19 ± 0.10 <sup>c</sup>	12.93 ± 0.06 <sup>b</sup>	18.17 ± 0.16 <sup>d</sup>	5.61 ± 0.06 <sup>c</sup>	2.89 ± 0.04 <sup>b</sup>	
IF	1.02 ± 0.03 <sup>d</sup>	3.39 ± 0.00 <sup>d</sup>	5.65 ± 0.02 <sup>a</sup>	5.97 ± 0.05 <sup>e</sup>	15.37 ± 0.02 <sup>a</sup>	18.63 ± 0.04 <sup>c</sup>	5.43 ± 0.01 <sup>d</sup>	3.40 ± 0.02 <sup>a</sup>	
SUIF	1.63 ± 0.02 <sup>b</sup>	3.73 ± 0.06 <sup>c</sup>	4.71 ± 0.08 <sup>d</sup>	5.61 ± 0.02 <sup>f</sup>	11.87 ± 0.19 <sup>c</sup>	20.36 ± 0.30 <sup>b</sup>	4.57 ± 0.06 <sup>f</sup>	2.27 ± 0.04 <sup>d</sup>	
DUIF	1.68 ± 0.03 <sup>a</sup>	4.19 ± 0.03 <sup>a</sup>	4.55 ± 0.01 <sup>e</sup>	11.39 ± 0.04 <sup>a</sup>	8.98 ± 0.04 <sup>e</sup>	22.06 ± 0.08 <sup>a</sup>	5.18 ± 0.05 <sup>e</sup>	2.61 ± 0.07 <sup>c</sup>	
TUIF	1.34 ± 0.01 <sup>c</sup>	3.90 ± 0.04 <sup>b</sup>	5.20 ± 0.02 <sup>b</sup>	8.44 ± 0.09 <sup>b</sup>	9.30 ± 0.02 <sup>d</sup>	20.35 ± 0.08 <sup>b</sup>	6.20 ± 0.04 <sup>b</sup>	3.21 ± 0.18 <sup>a</sup>	
	Ile	Leu	Tyr	Phe	Lys	His	Arg	Pro	Total
Fresh	4.50 ± 0.05 <sup>a</sup>	7.63 ± 0.10 <sup>b</sup>	3.45 ± 0.10 <sup>a</sup>	3.68 ± 0.10 <sup>a</sup>	14.41 ± 0.23 <sup>d</sup>	2.60 ± 0.04 <sup>d</sup>	0.01 ± 0.01 <sup>c</sup>	2.97 ± 0.11 <sup>a</sup>	91.26 ± 1.15 <sup>de</sup>
AF	3.84 ± 0.04 <sup>b</sup>	6.57 ± 0.07 <sup>c</sup>	2.76 ± 0.05 <sup>d</sup>	2.93 ± 0.03 <sup>c</sup>	12.59 ± 0.23 <sup>e</sup>	2.34 ± 0.04 <sup>e</sup>	0 ± 0 <sup>c</sup>	2.81 ± 2.12 <sup>a</sup>	89.60 ± 1.37 <sup>e</sup>
IF	3.76 ± 0.00 <sup>c</sup>	6.33 ± 0.02 <sup>d</sup>	3.34 ± 0.02 <sup>a</sup>	3.18 ± 0.01 <sup>b</sup>	20.81 ± 0.08 <sup>c</sup>	3.97 ± 0.02 <sup>b</sup>	0.03 ± 0.00 <sup>c</sup>	2.55 ± 0.85 <sup>a</sup>	102.81 ± 0.62 <sup>b</sup>
SUIF	2.97 ± 0.03 <sup>d</sup>	5.12 ± 0.07 <sup>e</sup>	2.11 ± 0.03 <sup>e</sup>	2.55 ± 0.04 <sup>d</sup>	22.44 ± 0.33 <sup>b</sup>	3.65 ± 0.05 <sup>c</sup>	0.21 ± 0.01 <sup>a</sup>	1.73 ± 0.11 <sup>a</sup>	94.93 ± 1.15 <sup>c</sup>
DUIF	3.82 ± 0.04 <sup>bc</sup>	6.37 ± 0.08 <sup>d</sup>	2.91 ± 0.08 <sup>c</sup>	2.88 ± 0.17 <sup>c</sup>	9.87 ± 0.17 <sup>f</sup>	2.62 ± 0.05 <sup>d</sup>	0.05 ± 0.00 <sup>b</sup>	3.14 ± 0.05 <sup>a</sup>	92.28 ± 0.77 <sup>d</sup>
TUIF	4.54 ± 0.02 <sup>a</sup>	8.12 ± 0.03 <sup>a</sup>	3.10 ± 0.03 <sup>b</sup>	3.00 ± 0.03 <sup>bc</sup>	28.57 ± 0.20 <sup>a</sup>	4.53 ± 0.04 <sup>a</sup>	0.21 ± 0.00 <sup>a</sup>	2.99 ± 0.03 <sup>a</sup>	112.00 ± 0.79 <sup>a</sup>

Fresh, fresh fish meat; AF, air freezing; IF, immersion freezing; SUIF, single-ultrasound assisted freezing; DUIF, dual-ultrasound assisted freezing; TUIF, triple-ultrasound assisted freezing. The means in the same column with different letters differ significantly ( $p < 0.05$ ).

samples. The most enriched FAAs in fresh and frozen samples were alanine, followed by lysine and glycine (Table 2). Aspartic acid, glutamic acid, alanine, and glycine provide the umami-sweetness taste in aquatic products. The UIF samples had higher alanine contents than the AF and IF samples, and TUIF samples showed the highest alanine content (20.35 mg/100 g). When the frequency is lower than 40 kHz, the cavitation intensity gets stronger with the increase in the frequency. Therefore, triple-frequency ultrasound can produce greater cavitation intensity than single-frequency and dual-frequency ultrasound (53). In the present study, histidine accounted for 2.61–4.04 mg/100 g of the total FAAs among all samples (Table 2). A low histidine content of (<5 mg/100 g) in large yellow croaker was recorded, which agreed with the results reported by Dou et al. (54) for large yellow croaker. Furthermore, the histidine content in large yellow croaker was much lower than that in other fish, such as silver carp (36.5 mg/100 g) (55) and grass carp (178.4 mg/100 g) (27). In summary, the results mentioned above indicated that flavour deterioration was associated with the decrease in special flavour-enhancing amino acids and the accumulation of flavour-detracting amino acids, and UIF treatment effectively delayed this process and maintained the good edible value of large yellow croaker during freezing.

## MP Primary Structure

### Changes in Total Sulfhydryl Content

Changes in sulfhydryl content can indicate changes in protein folding, disulfide bond formation, and protein conformation (56). All samples had a decreased total sulfhydryl content compared with the fresh sample (Figure 3B). Oxidation of proteins can result in the creation of disulfide bonds due to the oxidation of some reactive sulfhydryl groups during freezing, thereby leading to a decrease in the total sulfhydryl group content (57). The total sulfhydryl group content gradually increased

in the UIF samples with increasing ultrasound frequency, and the highest total sulfhydryl group content (85.09  $\mu\text{mol/g}$ ) was found in the TUIF sample. Zou et al. (58) found that the sulfhydryl content of ultrasonically treated chicken plasma protein increased significantly ( $p < 0.05$ ) compared with that of non-treated samples. The increase in total sulfhydryl groups may presume that the cavitation effect generated from ultrasonic treatment can disrupt disulfide bonds during processing as a result of the interaction of microstreaming, shear forces, and turbulence (59). However, Sun et al. (16) reported that UAF at different power levels showed a significant difference ( $p > 0.05$ ) in total sulfhydryl content, probably a result of the short freezing time.

### Changes in Carbonyl Contents

The carbonyl content in fresh large yellow croaker was 2.34 nmol/mg (Figure 3C), and all samples showed an increase after freezing treatment. The UAF samples had lower carbonyl contents than the AF and IF samples, and TUIF had the lowest carbonyl content (2.59 nmol/mg). Amino acids, such as lysine, proline, and arginine, are prone to be oxidised to a semialdehyde in the presence of metal ions and reactive oxygen species (ROS), accounting for ~70% of the total quantity of carbonyl groups. Due to the cavitation effect, ultrasound treatment stimulates chemical responses resulting in the production of highly reactive free radicals, which can cause the thermal decomposition of water molecules into  $\cdot\text{OH}$ ,  $\cdot\text{H}$ , and hydrogen peroxide (60). Additionally, lipid peroxides (carbonyl compounds and malondialdehyde) probably interact with proteins, generating carbonyl groups. This could be an explanation for the increase in the carbonyl concentration among all samples following the freezing process. However, the myofibril oxidation values of the UAF samples were clearly lower, demonstrating that the utilisation of ultrasound can effectually

inhibit the myofibril oxidation of large yellow croaker samples. Sun et al. (16) also reported that the carbonyl content was notably higher ( $p < 0.05$ ) in the high ultrasound power (UIF-200 and UIF-225) group than in the control group ( $p < 0.05$ ). However, Shi et al. (60) stated that there were no significant changes ( $p > 0.05$ ) in the carbonyl content in UAF grass carp samples.

## MP Secondary Structure

Fourier transform infrared spectroscopy is a widely applied means for evaluating the secondary structure of MPs, including  $\alpha$ -helices,  $\beta$ -turns,  $\beta$ -sheets, and random coils (61). The amide I region (1,700 to 1,600  $\text{cm}^{-1}$ ) is commonly applied for estimating MP secondary structure (Figure 3D). The fresh large yellow croaker samples contained 48.71%  $\alpha$ -helices, 24.87%  $\beta$ -sheets, 15.61%  $\beta$ -turns, and 10.81% random coils (Figure 3E). The second-derivative-fitted curve of the amide I band of MP is shown in Figure 3F. All samples exhibited a decline in  $\alpha$ -helical contents and a rise in  $\beta$ -sheet contents after the freezing treatments compared with the fresh sample. The content of  $\alpha$ -helices in the UIF samples was higher than that in the AF (39.22 %) and IF (41.21 %) samples, and TUIF had the highest proportion of  $\alpha$ -helices (43.30 %). The cavitation bubbles and microstreaming effects generated by trifrequency ultrasonic treatment accelerated the freezing process, resulting in the development of fine and well-distributed ice crystals, which decreased the damage to the fish muscles caused by the ice crystals. Stathopoulos et al. (62) stated that ultrasonic treatment induced a decline in  $\alpha$ -helix content together with a rise in the  $\beta$ -sheet structure of MPs. In contrast, Chandrapala et al. (63) found that ultrasound treatment (20 kHz, 450 W) resulted in a 10% gain in the  $\alpha$ -helix component and a 6–9% decrease in the  $\beta$ -sheet contents of whey protein concentrate. The FTIR results in this research indicated that freezing and ultrasonic treatment both affected the MP secondary structure, and that multifrequency ultrasound (especially TUIF) can decrease the changes in MP secondary structure resulting from freezing.

## MP Tertiary Structure

Intrinsic fluorescence intensity reflects the variations in MP tertiary structure (64). In general, tryptophan is in a non-polar environment if the  $\lambda_{\text{max}}$  is lower than 330 nm, whereas tryptophan is in a polar environment if the  $\lambda_{\text{max}}$  is higher than 330 nm (65). In this study, the fresh large yellow croaker samples revealed a  $\lambda_{\text{max}}$  value of 336.2 nm (Figure 3G), suggesting that tryptophan residues were in a polar atmosphere. The freezing process resulted in a transition of  $\lambda_{\text{max}}$  to longer wavelengths, ranging from 336.2 nm (fresh) to 337.3 nm (AF), demonstrating that parts of the buried tryptophan residues were exposed to a polar environment. These variations may be due to the different energy transfer efficiencies between tryptophan and tyrosine or exposure of the sample chromophore to solvent following freezing (66). No significant differences were observed in the  $\lambda_{\text{max}}$  values in samples ( $p > 0.05$ ). The samples with UIF treatment had lower  $\lambda_{\text{max}}$  values than the samples with AF and IF treatment, which may be due to the larger ice crystals induced by AF and IF, which destroyed the muscle properties. Zhang et al. (67) pointed out that samples that

underwent freeze-thaw treatment exhibited an increased  $\text{FI}_{\text{max}}$  compared to fresh samples, which might be due to protein–protein association induced by the freezing–thawing process. However, Wang et al. (22) stated that the IFI of MPs with different thawing methods was lower than that of fresh samples because of the unfolding of the MPs during rapid freezing and thawing. The IFI of the TUIF samples was significantly ( $p < 0.05$ ) larger than those of the DUIF and SUIF samples. This is probably because triple-frequency ultrasound has a significant effect on the MP structure by producing resonance with its own frequencies of MP. The resonance can cause a stronger effect on the MP samples, and thus the tertiary structure of MP was improved (44). Thus, multifrequency ultrasonic treatment accelerated freezing and reduced the destruction of muscle properties caused by ice crystals (38). The outcomes were further validated by microstructure observations, suggesting that multifrequency ultrasonic treatment can decrease injury to frozen fish tissue.

## CONCLUSIONS

This study investigated the influence of multifrequency ultrasonic treatments on the flavour attributes and MP characteristics of large yellow croaker. Multifrequency ultrasound slowed the accumulation of TVB-N in large yellow croaker during freezing process. The SEM images showed that multifrequency ultrasound contributed to the generation of finer and more uniform ice crystals to reduce muscle tissue damage. These effects become more obvious as the ultrasonic frequency increased. The quality of the samples frozen by TUIF was found to be better than that of the samples frozen by SUIF and DUIF. The formation of undesirable volatile flavour compounds was also inhibited by multifrequency ultrasonic treatment. The structure of multifrequency ultrasound samples was more stable than that of the AF and IF samples according to the FTIR and fluorescence spectra. These results indicated that multifrequency ultrasonic treatment efficiently improved the flavour attributes and MP characteristics of large yellow croaker. Therefore, multifrequency UAF is a promising food engineering technology to build sustainable and resilient food systems, improve nutritional profile of foods, and increase food and nutrition security.

## DATA AVAILABILITY STATEMENT

The raw data supporting the conclusions of this article will be made available by the authors, without undue reservation.

## ETHICS STATEMENT

Ethical review and approval was not required for the animal study because this study did not involve in live animal experiments.

## AUTHOR CONTRIBUTIONS

XM and JM: conceptualization and writing the original draft preparation. DY and WQ: methodology. XM and

WQ: data curation. JM and JX: writing, reviewing, and editing. DY and JX: funding acquisition. All authors contributed to the article and approved the submitted version.

## FUNDING

This research was funded by the National Key R&D Program of China (2019YFD0901603).

## REFERENCES

- Zhang P, Zhu Z, Sun DW. Using power ultrasound to accelerate food freezing processes: effects on freezing efficiency and food microstructure. *Crit Rev Food Sci Nutr.* (2018) 58:2842–53. doi: 10.1080/10408398.2018.1482528
- Hong GP, Choi MJ. Comparison of the quality characteristics of abalone processed by high-pressure sub-zero temperature and pressure-shift freezing. *Innovative Food Sci Emerging Technol.* (2016) 33:19–25. doi: 10.1016/j.ifset.2015.12.024
- Giddings GG, Hill LH. Relationship of freezing preservation parameters to texture-related structural damage to thermally processed crustacean muscle. *J Food Process Preserv.* (1978) 2:249–64. doi: 10.1111/j.1745-4549.1978.tb00561.x
- Anese M, Manzocco L, Panozzo A, Beraldo P, Foschia M, Nicoli MC. Effect of radiofrequency assisted freezing on meat microstructure and quality. *Food Res Int.* (2012) 46:50–4. doi: 10.1016/j.foodres.2011.11.025
- Cheng L, Sun DW, Zhu Z, Zhang Z. Effects of high pressure freezing (HPF) on denaturation of natural actomyosin extracted from prawn (*Metapenaeus ensis*). *Food Chem.* (2017) 229:252–9. doi: 10.1016/j.foodchem.2017.02.048
- Zhang C, Sun Q, Chen Q, Kong B, Diao X. Effects of ultrasound-assisted immersion freezing on the muscle quality and physicochemical properties of chicken breast. *Int J Refrig.* (2020) 117:247–55. doi: 10.1016/j.ijrefrig.2020.05.006
- Cheng X, Zhang M, Adhikari B, Islam MN, Xu B. Effect of ultrasound irradiation on some freezing parameters of ultrasound-assisted immersion freezing of strawberries. *Int J Refrig.* (2014) 44:49–55. doi: 10.1016/j.ijrefrig.2014.04.017
- Xu B, Zhang M, Bhandari B, Cheng X, Islam MN. Effect of ultrasound-assisted freezing on the physico-chemical properties and volatile compounds of red radish. *Ultrason Sonochem.* (2015) 27:316–24. doi: 10.1016/j.ultsonch.2015.04.014
- Islam MN, Zhang M, Adhikari B. Ultrasound-assisted freezing of fruits and vegetables: design, development, and applications. *Global Food Secur Wellness.* (2017) 457–87. doi: 10.1007/978-1-4939-6496-3\_22
- Islam MN, Zhang, Fang Z, Sun J. Direct contact ultrasound assisted freezing of mushroom (*Agaricus bisporus*): growth and size distribution of ice crystals. *Int J Refrig.* (2015) 57:46–53. doi: 10.1016/j.ijrefrig.2015.04.021
- Islam MN, Zhang, Adhikari B, Cheng X, Xu B. The effect of ultrasound-assisted immersion freezing on selected physicochemical properties of mushrooms. *Int J Refrig.* (2014) 42:121–33. doi: 10.1016/j.ijrefrig.2014.02.012
- Astráin-Redín L, Alejandre M, Raso J, Cebrián G, Álvarez I. Direct contact ultrasound in food processing: impact on food quality. *Front Nutr.* (2021) 8:633070. doi: 10.3389/fnut.2021.633070
- Nikmaram N, Rosentrater KA. Overview of some recent advances in improving water and energy efficiencies in food processing factories. *Front Nutr.* (2019) 6:20. doi: 10.3389/fnut.2019.00020
- Ma X, Mei J, Xie J. Mechanism of ultrasound assisted nucleation during freezing and its application in food freezing process. *Int J Food Prop.* (2021) 24:68–88. doi: 10.1080/10942912.2020.1858862
- Chow R, Blindt R, Chivers R, Povey M. A study on the primary and secondary nucleation of ice by power ultrasound. *Ultrasonics.* (2005) 43:227–30. doi: 10.1016/j.ultras.2004.06.006
- Sun Q, Chen Q, Xia X, Kong B, Diao X. Effects of ultrasound-assisted freezing at different power levels on the structure and thermal stability of common carp (*Cyprinus carpio*) proteins. *Ultrason Sonochem.* (2019) 54:311–20. doi: 10.1016/j.ultsonch.2019.01.026
- Xu B, Yuan J, Wang L, Lu F, Wei B, Azam RSM, et al. Effect of multi-frequency power ultrasound (MFPU) treatment on enzyme hydrolysis of casein. *Ultrason Sonochem.* (2020) 63:104930. doi: 10.1016/j.ultsonch.2019.104930
- Xu B, Chen J, Tiliwa ES, Yan W, Azam SMR, Yuan J, et al. Effect of multi-mode dual-frequency ultrasound pretreatment on the vacuum freeze-drying process and quality attributes of the strawberry slices. *Ultrason Sonochem.* (2021) 78:105714. doi: 10.1016/j.ultsonch.2021.105714
- Hasanzadeh H, Mokhtari-Dizaji M, Bathaie SZ, Hassan ZM, Nilchiani V, Goudarzi H. Enhancement and control of acoustic cavitation yield by low-level dual frequency sonication: a subharmonic analysis. *Ultrason Sonochem.* (2011) 18:394–400. doi: 10.1016/j.ultsonch.2010.07.005
- Ma H, Huang L, Peng L, Wang Z, Yang Q. Pretreatment of garlic powder using sweep frequency ultrasound and single frequency counter-current ultrasound: optimization and comparison for ACE inhibitory activities. *Ultrason Sonochem.* (2015) 21:109–15. doi: 10.1016/j.ultsonch.2014.10.020
- Jawale RH, Gogate PR, Pandit AB. Treatment of cyanide containing wastewater using cavitation based approach. *Ultrason Sonochem.* (2014) 21:1392–9. doi: 10.1016/j.ultsonch.2014.01.025
- Wang YY, Rashid MT, Yan JK, Ma H. Effect of multi-frequency ultrasound thawing on the structure and rheological properties of myofibrillar proteins from small yellow croaker. *Ultrason Sonochem.* (2021) 70:105352. doi: 10.1016/j.ultsonch.2020.105352
- Li B, Sun DW. Effect of power ultrasound on freezing rate during immersion freezing of potatoes. *J Food Eng.* (2002) 55:277–82. doi: 10.1016/S0260-8774(02)00102-4
- Ma X, Mei J, Xie J. Effects of multi-frequency ultrasound on the freezing rates, quality properties and structural characteristics of cultured large yellow croaker (*Larimichthys crocea*). *Ultrason Sonochem.* (2021) 76:105657. doi: 10.1016/j.ultsonch.2021.105657
- Liu W, Wang Q, Mei J, Xie J. Shelf-life extension of refrigerated turbot (*Scophthalmus maximus*) by using weakly acidic electrolyzed water and active coatings containing daphnetin emulsions. *Front Nutr.* (2021) 8:696212. doi: 10.3389/fnut.2021.696212
- Li N, Liu W, Shen Y, Mei J, Xie J. Coating effects of  $\epsilon$ -polylysine and rosmarinic acid combined with chitosan on the storage quality of fresh half-smooth tongue sole (*Cynoglossus semilaevis Günther*) filets. *Coatings.* (2019) 9:273. doi: 10.3390/coatings9040273
- Yu D, Xu Y, Regenstein JM, Xia W, Yang F, Jiang Q, et al. The effects of edible chitosan-based coatings on flavor quality of raw grass carp (*Ctenopharyngodon idellus*) filets during refrigerated storage. *Food Chem.* (2018) 242:412–20. doi: 10.1016/j.foodchem.2017.09.037
- Guo Y, Kong B, Xia X, Yu T, Liu Q. Changes in physicochemical and protein structural properties of common carp (*Cyprinus carpio*) muscle subjected to different freeze-thaw cycles. *J Aquat Food Prod Technol.* (2014) 23:579–90. doi: 10.1080/10498850.2012.741663
- Li P, Mei J, Xie J. Chitosan-sodium alginate bioactive coatings containing  $\epsilon$ -polylysine combined with high CO<sub>2</sub> modified atmosphere packaging inhibit myofibril oxidation and degradation of farmed pufferfish (*Takifugu obscurus*) during cold storage. *LWT-Food Sci Technol.* (2021) 140:110652. doi: 10.1016/j.lwt.2020.110652
- Zhang L, Li Q, Hong H, Luo Y. Prevention of protein oxidation and enhancement of gel properties of silver carp (*Hypophthalmichthys molitrix*) surimi by addition of protein hydrolysates derived from surimi processing by-products. *Food Chem.* (2020) 316:126343. doi: 10.1016/j.foodchem.2020.126343

31. Liu W, Mei J, Xie J. Effect of locust bean gum-sodium alginate coatings incorporated with daphnetin emulsions on the quality of *Scophthalmus maximus* at refrigerated condition. *Int J Biol Macromol.* (2021) 170:129–39. doi: 10.1016/j.ijbiomac.2020.12.089
32. Cao X, Islam MN, Duan Z, Pan X, Xu W, Wei X, et al. Chlorogenic acid osmosis of snakehead fish: a novel approach to maintain quality and suppress deterioration during storage. *Int. J Food Prop.* (2020) 23:387–99. doi: 10.1080/10942912.2020.1732409
33. Cao X, Islam MN, Chitrakar B, Duan Z, Xu W, Zhong S. Effect of combined chlorogenic acid and chitosan coating on antioxidant, antimicrobial, and sensory properties of snakehead fish in cold storage. *Food Sci Nutr.* (2020) 8:973–81. doi: 10.1002/fsn3.1378
34. Vacha F, Cepak M, Urbanek M, Vejsada P, Hartvich P, Rost M. Impact of long-term storage on the instrumental textural properties of frozen common carp (*Cyprinus carpio*, L) flesh. *Int J Food Prop.* (2013) 16:241–50. doi: 10.1080/10942912.2010.551309
35. Xu B, Chen J, Azam SMR, Feng M, Wei B, Yan W, et al. Flat dual-frequency sweeping ultrasound enhances the inactivation of polyphenol oxidase in strawberry juice. *J Food Meas Charact.* (2021). doi: 10.1007/s11694-021-01202-3
36. Sun Q, Sun F, Xia X, Xu H, Kong B. The comparison of ultrasound-assisted immersion freezing, air freezing and immersion freezing on the muscle quality and physicochemical properties of common carp (*Cyprinus carpio*) during freezing storage. *Ultrason Sonochem.* (2019) 51:281–91. doi: 10.1016/j.ultsonch.2018.10.006
37. Kiani H, Zhang Z, Delgado A, Sun DW. Ultrasound assisted nucleation of some liquid and solid model foods during freezing. *Food Res Int.* (2011) 44:2915–21. doi: 10.1016/j.foodres.2011.06.051
38. Zhang M, Niu H, Chen Q, Xia X, Kong B. Influence of ultrasound-assisted immersion freezing on the freezing rate and quality of porcine longissimus muscles. *Meat Sci.* (2018) 136:1–8. doi: 10.1016/j.meatsci.2017.10.005
39. Panzella L, Moccia F, Nasti R, Marzorati S, Verotta L, Napolitano A. Bioactive phenolic compounds from agri-food wastes: an update on green and sustainable extraction methodologies. *Front Nutr.* (2020) 7:60. doi: 10.3389/fnut.2020.00060
40. Zhu Z, Zhang P, Sun DW. Effects of multi-frequency ultrasound on freezing rates and quality attributes of potatoes. *Ultrason Sonochem.* (2020) 60:104733. doi: 10.1016/j.ultsonch.2019.104733
41. Feng R, Zhao Y, Zhu C, Mason TJ. Enhancement of ultrasonic cavitation yield by multi-frequency sonication. *Ultrason Sonochem.* (2002) 9:231–6. doi: 10.1016/S1350-4177(02)00083-4
42. Jin J, Ma H, Qu W, Wang K, Zhou C, He R, et al. Effects of multi-frequency power ultrasound on the enzymolysis of corn gluten meal: kinetics and thermodynamics study. *Ultrason Sonochem.* (2015) 27:46–53. doi: 10.1016/j.ultsonch.2015.04.031
43. Iglesias J, Medina I, Bianchi F, Careri M, Mangia A, Musci M. Study of the volatile compounds useful for the characterisation of fresh and frozen-thawed cultured gilthead sea bream fish by solid-phase microextraction gas chromatography–mass spectrometry. *Food Chem.* (2009) 115:1473–8. doi: 10.1016/j.foodchem.2009.01.076
44. Xu B, Ren A, Chen J, Li H, Wei B, Wang J, et al. Effect of multi-mode dual-frequency ultrasound irradiation on the degradation of waxy corn starch in a gelatinized state. *Food Hydrocolloids.* (2021) 113:106440. doi: 10.1016/j.foodhyd.2020.106440
45. Alasalvar C, Taylor KDA, Shahidi F. Comparison of volatiles of cultured and wild sea bream (*Sparus aurata*) during storage in ice by dynamic headspace analysis/gas chromatography-mass spectrometry. *J Agric Food Chem.* (2005) 53:2616–22. doi: 10.1021/jf0483826
46. Li Q, Zhang L, Luo Y. Changes in microbial communities and quality attributes of white muscle and dark muscle from common carp (*Cyprinus carpio*) during chilled and freeze-chilled storage. *Food Microbiol.* (2018) 73:237–44. doi: 10.1016/j.fm.2018.01.011
47. Tan X, Qi L, Fan F, Guo Z, Wang Z, Song W, et al. Analysis of volatile compounds and nutritional properties of enzymatic hydrolysate of protein from cod bone. *Food Chem.* (2018) 264:350–7. doi: 10.1016/j.foodchem.2018.05.034
48. Fernández-Segovia I, Escriche I, Gómez-Sintes M, Fuentes A, Serra JA. Influence of different preservation treatments on the volatile fraction of desalted cod. *Food Chem.* (2006) 98:473–82. doi: 10.1016/j.foodchem.2005.06.021
49. Kawai T, Sakaguchi M. Fish flavor. *Crit Rev Food Sci Nutr.* (1996) 36:257–98. doi: 10.1080/10408399609527725
50. Yang Y, Sun Y, Pan D, Wang Y, Cao J. Effects of high pressure treatment on lipolysis-oxidation and volatiles of marinated pork meat in soy sauce. *Meat Sci.* (2018) 145:186–94. doi: 10.1016/j.meatsci.2018.06.036
51. Jónsdóttir R, Ólafsdóttir G, Chanie E, Haugen JE. Volatile compounds suitable for rapid detection as quality indicators of cold smoked salmon (*Salmo salar*). *Food Chem.* (2008) 109:184–95. doi: 10.1016/j.foodchem.2007.12.006
52. Osako K, Fujii A, Ruttanapornvareesakul Y, Nagano N, Kuwahara K, Okamoto A. Differences in free amino acid composition between testis and ovary of sea urchin *Anthocidaris crassispina* during gonadal development. *Fish Sci.* (2007) 73:660–7. doi: 10.1111/j.1444-2906.2007.01379.x
53. Zhang L, Zhou C, Wang B, Yagoub AEGA, Ma H, Zhang X, et al. Study of ultrasonic cavitation during extraction of the peanut oil at varying frequencies. *Ultrason Sonochem.* (2017) 37:106–13. doi: 10.1016/j.ultsonch.2016.12.034
54. Dou X, Wang YQ, Wu YY, Hu X, Yang, SL, et al. Analysis and evaluation of nutritional components in liver of large yellow croaker (*Pseudosciaena crocea*). *CyTA–J Food.* (2020) 18:551–60. doi: 10.1080/19476337.2020.1800824
55. Shi C, Cui J, Qin N, Luo Y, Lu H, Wang H. Effect of ginger extract and vinegar on ATP metabolites, IMP-related enzyme activity, reducing sugars and phosphorylated sugars in silver carp during postslaughter storage. *Int J Food Sci Technol.* (2017) 52:413–23. doi: 10.1111/ijfs.13296
56. Li H, Zhao T, Li H, Yu J. Effect of heat treatment on the property, structure, and aggregation of skim milk proteins. *Front Nutr.* (2021) 8:714869. doi: 10.3389/fnut.2021.714869
57. Nikoo M, Benjakul S, Xu X. Antioxidant and cryoprotective effects of Amur sturgeon skin gelatin hydrolysate in unwashed fish mince. *Food Chem.* (2015) 181:295–303. doi: 10.1016/j.foodchem.2015.02.095
58. Zou Y, Yang H, Li PP, Zhang MH, Zhang XX, Xu WM, et al. Effect of different time of ultrasound treatment on physicochemical, thermal, and antioxidant properties of chicken plasma protein. *Poult Sci.* (2019) 98:1925–33. doi: 10.3382/ps/pey502
59. Jin J, Ma H, Wang K, Yagoub AEGA, Owusu J, Qu W, et al. Effects of multi-frequency power ultrasound on the enzymolysis and structural characteristics of corn gluten meal. *Ultrason Sonochem.* (2015) 24:55–64. doi: 10.1016/j.ultsonch.2014.12.013
60. Shi Z, Zhong S, Yan W, Liu M, Yang Z, Qiao X. The effects of ultrasonic treatment on the freezing rate, physicochemical quality, and microstructure of the back muscle of grass carp (*Ctenopharyngodon idella*). *LWT–Food Sci Technol.* (2019) 111:301–8. doi: 10.1016/j.lwt.2019.04.071
61. Arunkumar R, Drummond CJ, Greaves TL. FTIR spectroscopic study of the secondary structure of globular proteins in aqueous protic ionic liquids. *Front Chem.* (2019) 7:74. doi: 10.3389/fchem.2019.00074
62. Stathopoulos PB, Scholz GA, Hwang YM, Rumpfheldt JAO, Lepock JR, Meiering EM. Sonication of proteins causes formation of aggregates that resemble amyloid. *Protein Sci.* (2004) 13:3017–27. doi: 10.1110/ps.04831804
63. Chandrapala J, Zisu B, Palmer M, Kentish S, Ashokkumar M. Effects of ultrasound on the thermal and structural characteristics of proteins in reconstituted whey protein concentrate. *Ultrason Sonochem.* (2011) 18:951–7. doi: 10.1016/j.ultsonch.2010.12.016
64. Sun W, Zhao M, Yang B, Zhao H, Cui C. Oxidation of sarcoplasmic proteins during processing of Cantonese sausage in relation to their aggregation behaviour and in vitro digestibility. *Meat Sci.* (2011) 88:462–7. doi: 10.1016/j.meatsci.2011.01.027
65. Tang CH, Sun X, Foegeding EA. Modulation of physicochemical and conformational properties of kidney bean vicilin (phaseolin) by glycation with glucose: implications for structure–function relationships of legume vicilins. *J Agric Food Chem.* (2011) 59:10114–23. doi: 10.1021/jf202517f
66. Broersen K, Teeffelen AMMV, Vries A, Voragen AGJ, Hamer RJ, Jongh HHJD. Do sulfhydryl groups affect aggregation and gelation properties of ovalbumin? *J Agric Food Chem.* (2006) 54:5166–74. doi: 10.1021/jf0601923

67. Zhang Y, Ertbjerg P. On the origin of thaw loss: relationship between freezing rate and protein denaturation. *Food Chem.* (2019) 299:125104. doi: 10.1016/j.foodchem.2019.125104

**Conflict of Interest:** The authors declare that the research was conducted in the absence of any commercial or financial relationships that could be construed as a potential conflict of interest.

**Publisher's Note:** All claims expressed in this article are solely those of the authors and do not necessarily represent those of their affiliated organizations, or those of

the publisher, the editors and the reviewers. Any product that may be evaluated in this article, or claim that may be made by its manufacturer, is not guaranteed or endorsed by the publisher.

*Copyright © 2021 Ma, Yang, Qiu, Mei and Xie. This is an open-access article distributed under the terms of the Creative Commons Attribution License (CC BY). The use, distribution or reproduction in other forums is permitted, provided the original author(s) and the copyright owner(s) are credited and that the original publication in this journal is cited, in accordance with accepted academic practice. No use, distribution or reproduction is permitted which does not comply with these terms.*